Electronic Supplementary Information

De novo fabrication of multi-heteroatom-doped carbonaceous materials via an in situ doping strategy

Yali Luo,[a] Zhenzhen Yang,*[b,c] Wei Guo,[b] Hao Chen,[b] Tao Wang,[b] Yunfei Liu,[a] Yinong Lyu,[a] Huimin Luo,[c] and Sheng Dai,*[b,c]

[a] College of Materials Science and Engineering, Nanjing Tech University, Nanjing, 211816, PR China.
[b] Department of Chemistry, The University of Tennessee, Knoxville, TN, 37996, USA. Email: ZYANG17@utk.edu; dais@ornl.gov.
[c] Chemical Sciences Division, Oak Ridge National Laboratory, Oak Ridge, TN 37831, USA.

Table of contents

1 EXPERIMENTAL SECTION

1.1 Materials

Sodium tetrakis(1-imidazolyl)borate (NaBIm4), chloroacetonitrile, lithium bis(trifluoromethanesulfonyl)imide (LiTFSI), lithium bis (pentafluoroethylsulfonyl)imide (LiBETI), and anhydrous *N,N*-dimethylformamide (DMF) were purchased from Aladdin and Sinopharm Chemical and used without further purification. Methylene blue (MB) was purchased from Alfa-Aesar. The MB solution (50 μM) for adsorption test was prepared using de-ionized water. Ionic liquid 1,3-bis(cyanomethyl)imidazolium bis(trifluoromethanesulfonyl)imide ([BCNIm][TFSI]) and the derived porous carbon was synthesized according to the previous report.[1]

1.2 Synthesis of tetrakis(1-imidazolyl)borate-based ionic liquid

Tetrakis(1-imidazolyl) borate-based cationic liquids were synthesized by one-step quaternization of sodium tetrakis(1-imidazolyl)borate (NaBIm$_4$) with chloroacetonitrile, and successive anion exchange procedure. Typically, NaBIm$_4$ (1.80 g, 6 mmol) was dissolved in 50 mL of anhydrous DMF in a 200 ml Schlenk flask. After three vacuum/N$_2$ purge cycles, chloroacetonitrile (4.53 g, 60 mmol) was added and the mixture was heated to 100 °C for 72 h. The result solid product was isolated by centrifugation and washed with acetone. The product, denoted as NaBIm$_4$CH$_2$CNCl, was dried in vacuo at 40 °C more than 12 h. Successively, Na[(BIm$_4$-CH$_2$CN)$_4$Cl$_4$] (1.21 g, 2 mmol) was dissolved in water, followed by addition of Li(TFSI)$_4$ (2.30 g, 8 mmol) aqueous solution under vigorous stirring. A gray precipitate was immediately formed, and the mixture was further stirred overnight at room temperature. The suspension was isolated by centrifugation, washed with water. the solid product, denoted as Na[(BIm$_4$-CH$_2$CN)$_4$(TFSI)$_4$], was dried in vacuo for more than 12 h.

Similar to the preparation of Na[(BIm$_4$-CH$_2$CN)$_4$(TFSI)$_4$], Li(BETI)$_4$ (3.10 g, 8 mmol) was used to afford Na[(BIm$_4$-CH$_2$CN)$_4$(BETI)$_4$].

1.3 Preparation of carbon materials

Carbon materials were prepared by placing Na[(BIm$_4$-CH$_2$CN)$_4$(TFSI)$_4$] or Na[(BIm$_4$-CH$_2$CN)$_4$(BETI)$_4$] directly in an alumina crucible and carbonized in a tube furnace. The sample was heated at 10 °C/min under nitrogen flow to 600 °C and maintained at the final temperature for 1 h. After cooling down, the obtained black materials were ground into a powder for further experiments and analysis. The carbon yields are 29% and 33% for BNOFS-C-1 (carbon from Na[(BIm$_4$-CH$_2$CN)$_4$(TFSI)$_4$]) and BNOFS-C-2 (carbon from Na[(BIm$_4$-CH$_2$CN)$_4$(BETI)$_4$]), respectively. Elemental analysis (wt%): BNOFS-C-1: C, 45.96; H, 2.38; N, 29.49; F, 1.18. BNOFS-C-2: C, 47.58; H, 2.62; N, 26.14; F, 2.28.

1.4 Methylene blue adsorption experiment

All the adsorption experiments were conducted at room temperature. Typically, 10 mg of adsorbents (BNOFS-C-1 and BNOFS-C-2) was dispersed into 10 mL of MB solutions with a concentration of 0.05 mM. At appropriate time interval, the aliquots were taken from the mixture, and the adsorbents were separated by syringe filter (0.45 μm pore size, Nylon, Whatman). The dye concentration in the solutions was detected by UV absorbance at 664 nm. The percentage removal of MB was calculated by using the following equation,

$$\text{Removal percentage (\%)} = (C_0 - C_t)/C_0 \times 100 = (A_0 - A_t)/A_0 \times 100$$

Where C_0 and A_0 are initial concentration and absorbance of the MB solution, respectively. C_t and A_t are concentration and absorbance of the MB solution at specific times, respectively.

Adsorption of MnO_4^- (0.5 mM) ion and 4-nitropheno (4-NP, 0.05 mM) were conducted with the same procedure as that for MB.

1.5 Calculation of adsorption capacity

3 mg of BNOFS-C-1 was added into 10 mL of 0.1 mM MB solutions for 24 h at stirring condition. After centrifuge, the supernatant solution was subjected to UV-Vis measurements. The maximum adsorption capacity was calculated using the following equation,

$$C = (C_0 - C_t) \times V \times M_{dye}/m$$

Where C is the capacity of adsorbent, C_0 and C_t are the concentration of dyes at initial and final time, respectively. V is the volume of solution, M_{dye} is molecular weight of dye and m is the mass of porous carbon.

The adsorption capacity study of BNOFS-C-2 for MB was similar to that of BNOFS-C-1 for MB except the concentration and volume of MB solution are about 0.08 mM and 25 mL, respectively.

The adsorption capacity study of BNOFS-C-1 for MnO_4^- ion was similar to that of BNOFS-C-1 for MB except the concentration and volume of MnO_4^- solution are about 1 mM and 15 mL, respectively.

1.6 Characterization

FTIR spectra of the samples were collected on a Nicolet Is50 FTIR spectrometer in the 500-4000 cm^{-1} range. Liquid ^{1}H, ^{11}B, and ^{19}F NMR spectra was recorded on Bruck 400 MHz NMR spectrometer. For TGA analysis, samples were heated at 10°C mim^{-1} in open aluminum pans with a Discovery TGA (TA Instruments, Waters, LLC, USA). X-ray photoelectron spectroscopy (XPS) were performed with a PHI 3056 spectrometer using an Al radiation (350 W). Elemental analyses were performed by Atlantic Microlab Inc., Norcross, GA. Raman scattering spectra were taken on a Renishaw inVia, U.K. Powder X-ray diffraction (XRD) data were recorded with a PANalytical Empyrean diffractometer, operated at 45 kV and 40 mA (Scanning step: 0.04° per step). Field emission scanning electron microscopy (SEM) observations were performed on a Hitachi S-4800 microscope operated at an accelerating voltage of 15.0 kV. High resolution transmission electron microscopy (HRTEM) were conducted on an aberration-corrected FEI Titan S 80-300. TEM was operated at 300 kV and a large active area (60 mm^2). The adsorption/desorption isotherms were recorded on a Gemini 2360 surface area analyzer. The samples were outgassed at 150°C for 16 h before the measurements. The temperatures were maintained at 77 K in liquid nitrogen bath and 87 K in liquid argon bath. Surface areas were calculated from the adsorption data using Brunauer-Emmett-Teller (BET) methods. The pore size distribution curves were obtained from the adsorption branches using non-local density functional theory (NLDFT) method. The gas (CO_2 and N_2) adsorption isotherms were measured using Autosorb-1-C Quantachrome analyzer at both 273 and 298 K. To investigate the recyclability of the porous carbon materials in CO_2 capture, the used porous carbon was regenerated by evacuating at 160 °C overnight and then reused in CO_2 adsorption test. UV-vis spectra were recorded with an ultraviolet-visible spectrophotometer (Evolution 300, Scientific).

1.7 CO_2/N_2 selectivity calculation by the ideal adsorption solution theory (IAST)

The experimental adsorption isotherms were firstly fitted using the single-site Langmuir model:

$$q = q_{A,sat}[b_A p^{vA}/(1+b_A p^{VA})] + q_{B,sat}[b_B p^{VB}/(1+b_B p^{VB})]$$

where P (kPa) is the pressure of the bulk gas at equilibrium with the adsorbed phase; q (mol kg^{-1}) is the adsorbed amount at equilibrium; $q_{A,sat}$ and $q_{B,sat}$ (mol kg^{-1}) are the saturation capacities of sites A and B; b_A and b_B (kPa^{-vi}) are the affinity coefficients of sites A and B; and v_A and v_B are the Freundlich coefficients.

The adsorption selectivity for CO_2/N_2 separation was estimated using ideal adsorbed solution theory (IAST):

$$Sads = (x_i/x_j)/(y_i/y_j)$$

Where x_i and x_j are the adsorption capacity of components i and j, and y_i and y_j are the gaseous molar fractions of i and j.

Supplementary table and Fig. S

Table S1 Porosity parameters of the porous materials.

| materials	S_{BET}[a]	S_{micro}[b]	V_{total}[c]	V_{mico}[d]
BNOFS-C-1	593	321	0.29	0.13
BNOFS-C-2	1021	612	0.50	0.25

[a] Surface area (m^2 g^{-1}) calculated from the nitrogen adsorption branch according to the BET model. [b] Microporous surface area (m^2 g^{-1}) calculated using the t-plot method. [c] The total pore volume (cm^3 g^{-1}) calculated from single point nitrogen uptake at $P/P_0 = 0.95$. [d] Microporous volume (cm^3 g^{-1}) calculated using the t-plot method.

Table S2 Comparison of the maximum adsorption capacity of BNOFS-C-1 and BNOFS-C-2 for CO_2, MB, and MnO_4^- (this work), and other porous carbons documented in the literatures.

Adsorbate	Adsorbent	kind of heteroatoms	S_{BET} (m^2 g^{-1})	Max adsorption capacity[a]	Reference
CO_2	BNOFS-C-1	N, O, F, B	594	3.21	This work
	BNOFS-C-2	N, O, F, B	1021	3.96	This work
	[BCNIm][TFSI]	N, O, F	673	2.99	[1]
	NMC-7	N	481	1.64	[2]
	EBT-T	N, O, F	883	2.13	[3]
	Th850	S	2682	2.4	[4]
	Py800	N	4334	3.5	[4]
MB	BNOFS-C-1	N, O, F, B	594	46	This work
	BNOFS-C-2	N, O, F, B	1021	123	This work
	[BCNIm][TFSI]	N, O, F	673	49	[1]
	CTF-A	N	791	110	[5]
	AHCP-1	O, B	939	130	[6]
	Fe-impregnated AC	Fe	570	21	[7]
MnO_4^-	BNOFS-C-1	N, O, F, B	594	289	This work
	NH_2/MCM-41/NTAA	N	627	165	[8]
	Compound-1	N	/	297	[9]
	Surfactant modified smectite clay	/	14	111	[10]

[a] The CO_2 uptake capacity is measured at 273 K/1bar and the unit is mmol g^{-1}; for MB and MnO_4^- adsorption, the units is mg g^{-1}.
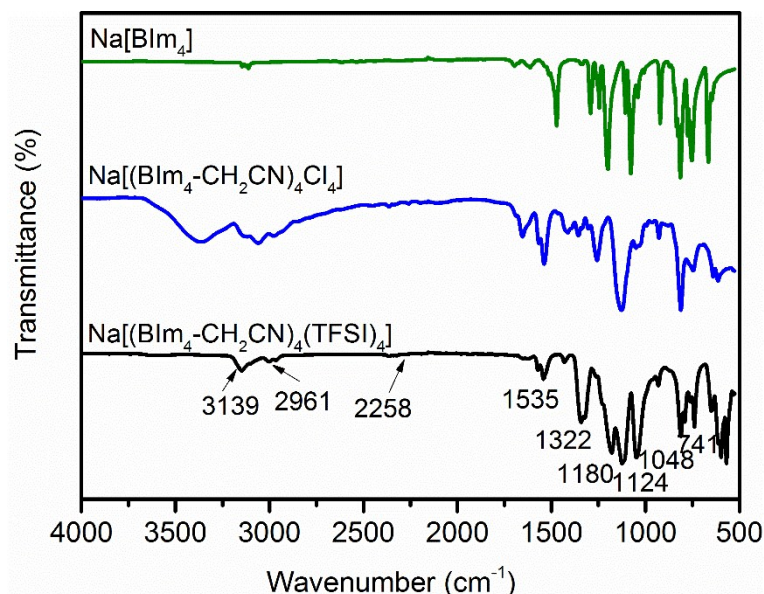
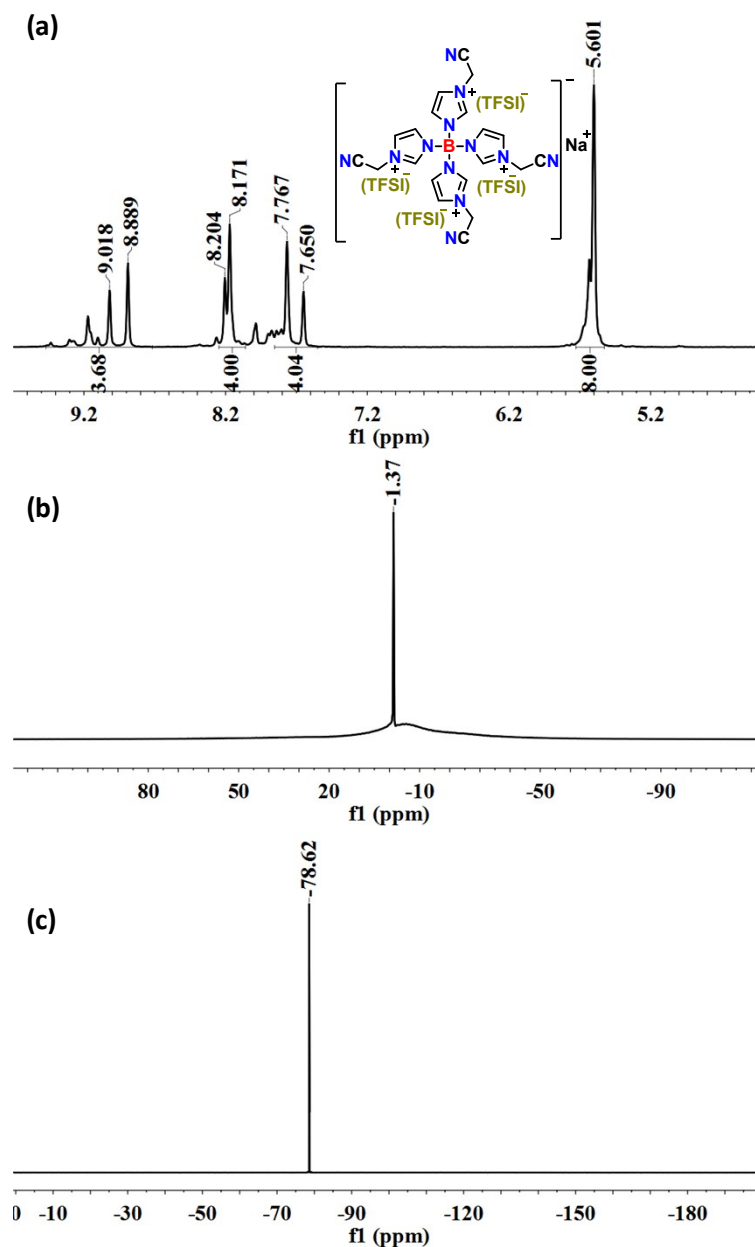**Fig. S1** FTIR spectra of Na[(BIm$_4$], Na[(BIm$_4$-CH$_2$CN)$_4$Cl$_4$], and Na[(BIm$_4$-CH$_2$CN)$_4$(TFSI)$_4$]. For Na[(BIm4-CH2CN)4(TFSI)4], 3139, 3074 (aromatic C-H), 2961 (aliphatic C-H), 2258 (C≡N). 1535 (imidazolium ring), 1322 (in-plane B-N), 1180 (asymmetric stretching vibration of S=O) 1124 (C-F) 1048 (symmetric stretching vibration of S=O), 774 (out-of-plane B-N-B).
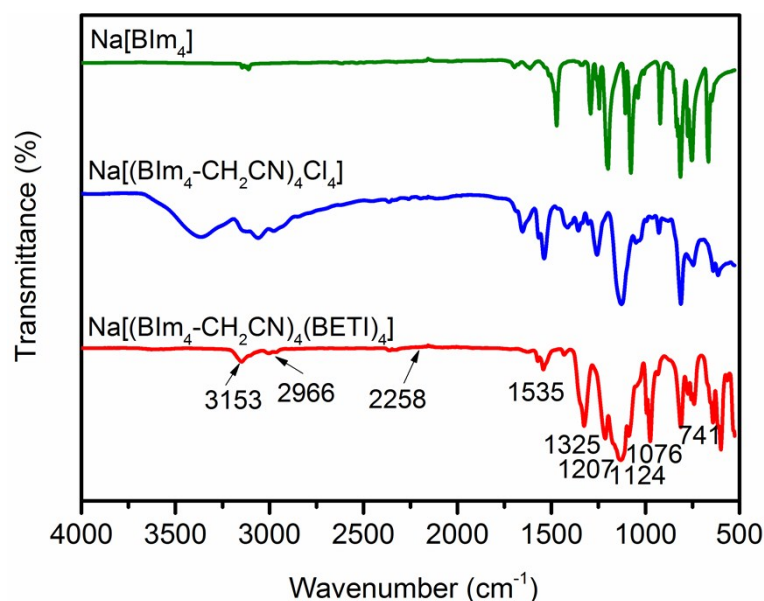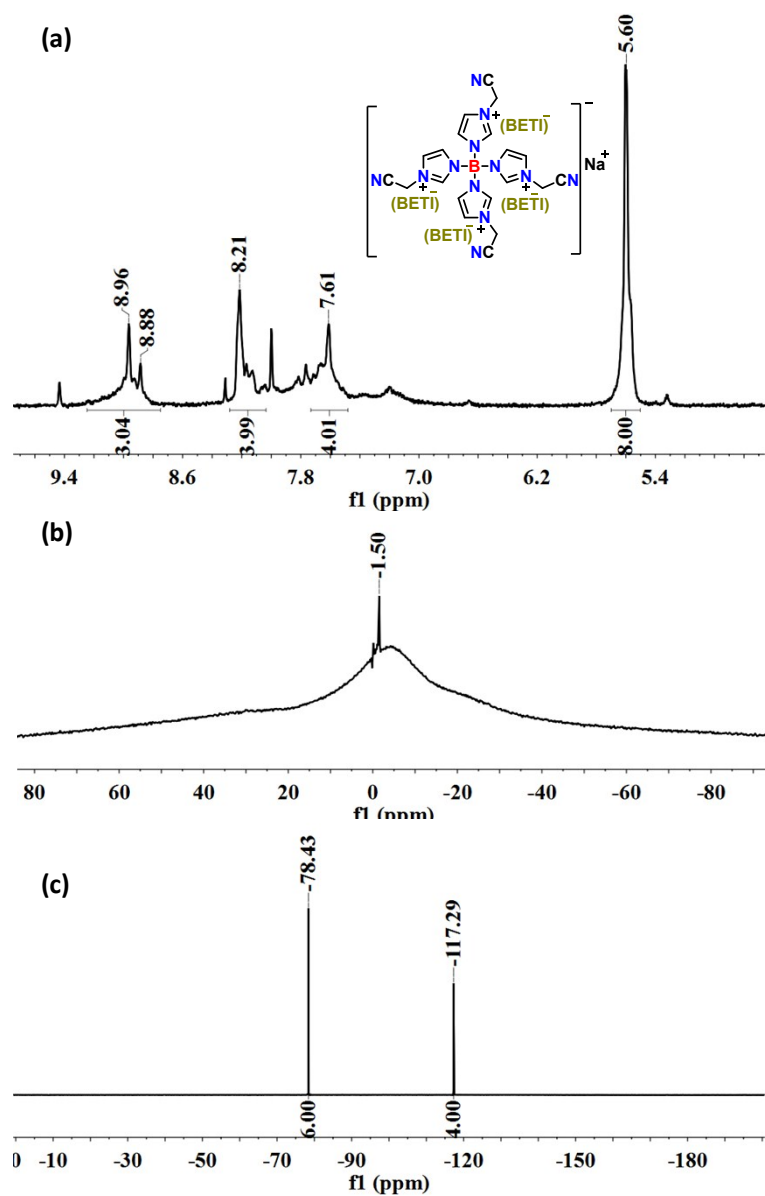

Fig. S2 FTIR spectra of Na[(BIm$_4$], Na[(BIm$_4$-CH$_2$CN)$_4$Cl$_4$], and Na[(BIm$_4$-CH$_2$CN)$_4$(BETI)$_4$]. For Na[(BIm$_4$-CH$_2$CN)$_4$(BETI)$_4$], 3153, 3102 (aromatic C-H), 2966 (aliphatic C-H), 2258 (C≡N). 1535 (imidazolium ring), 1325 (in-plane B-N), 1207 (asymmetric stretching vibration of S=O) 1124 (C-F) 1076 (symmetric stretching vibration of S=O), 774 (out-of-plane B-N-B)

Fig. S3 NMR spectra of Na[(BIm$_4$-CH$_2$CN)$_4$(TFSI)$_4$]. ^{1}H NMR (DMSO-d_6, 400 MHz): δ 8.95 (d, J = 51.5 Hz, 1H), 8.19 (d, J = 13.5 Hz, 1H), 7.71 (d, J = 46.6 Hz, 1H), 5.60 (s, 2H). ^{11}B NMR (DMSO-d_6, 128 MHz): δ -1.37 (s). ^{19}F-NMR: (DMSO-d_6, 376 MHz): δ -78.62 (s).

Fig. S4 NMR spectra of Na[(BIm$_4$-CH$_2$CN)$_4$(BETI)$_4$]. ^{1}H NMR (DMSO-d_6, 400 MHz) δ 8.92 (d, J = 31.4 Hz, 1H), 8.11 (d, J = 85.6 Hz, 1H), 7.69 (d, J = 62.7 Hz, 1H), 5.60 (s, 2H). ^{11}B NMR (DMSO-d_6,128 MHz) δ -1.50 (s). ^{19}F NMR (DMSO-d_6, 376 MHz) δ -78.43 (s), -117.29 (s).
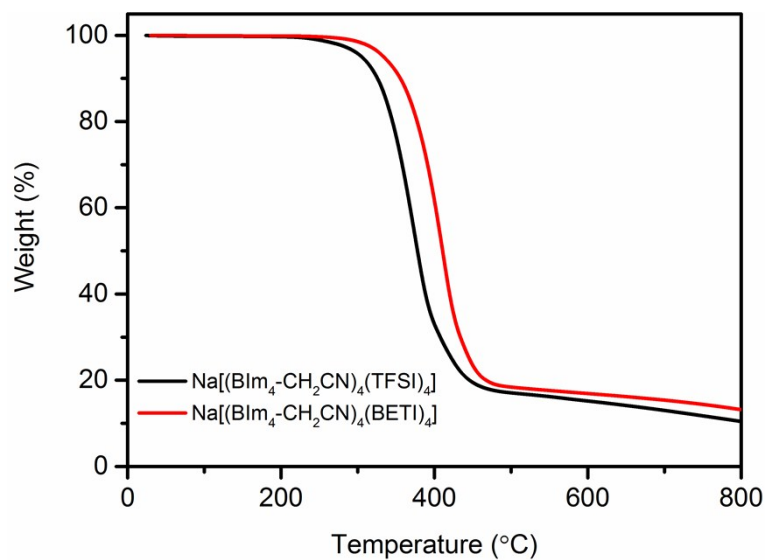
Fig. S5 Thermogravimetric analysis (TGA) curves of the ionic liquid precursors under N_2 atmosphere with a ramp rate of 10 °C min^{-1}.
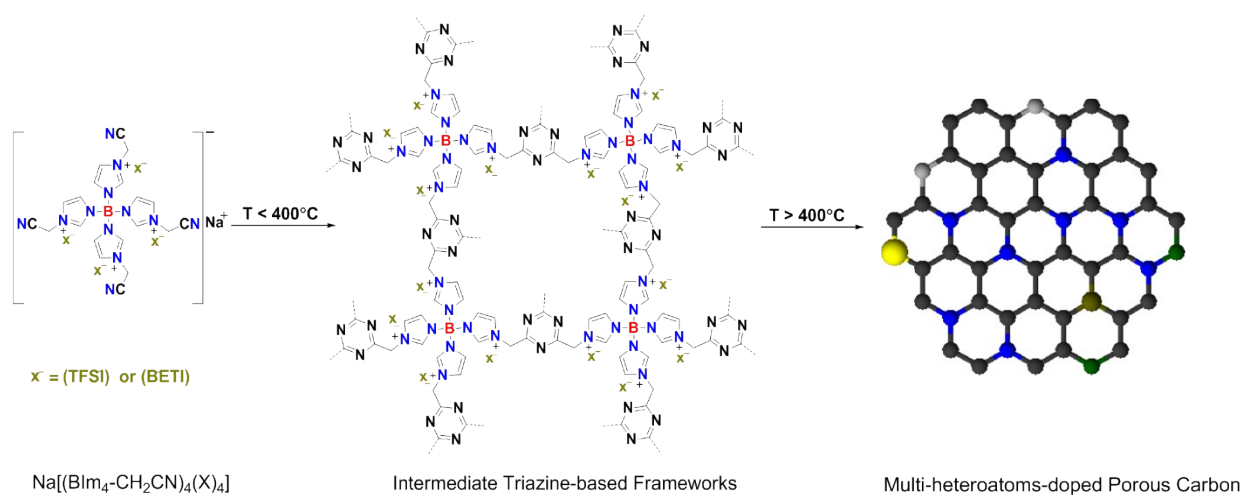

Fig. S6 Proposed reaction scheme for trimerization of nitrile-functionalized TSILs leading to intermediate triazine-based frameworks and the hypothetical chemical structure of the carbonaceous materials (C, black; N, blue; O, green; F, silver; S, yellow; B, olive).
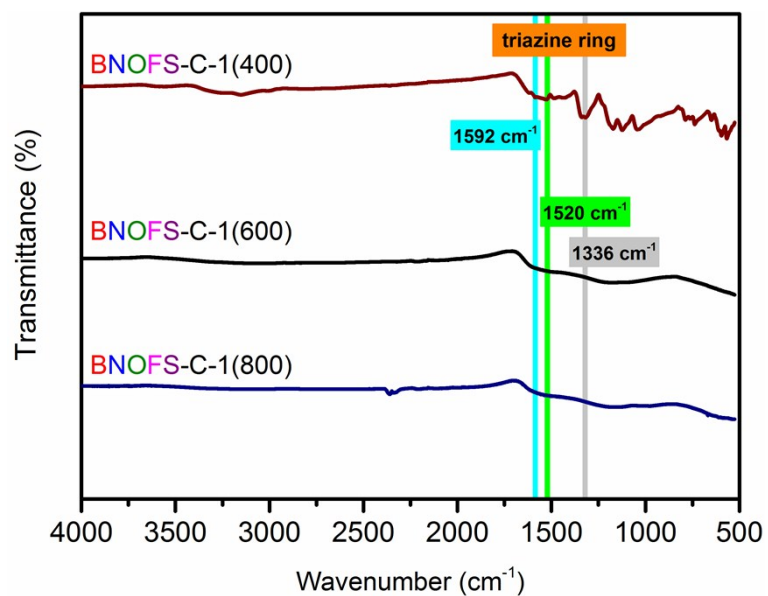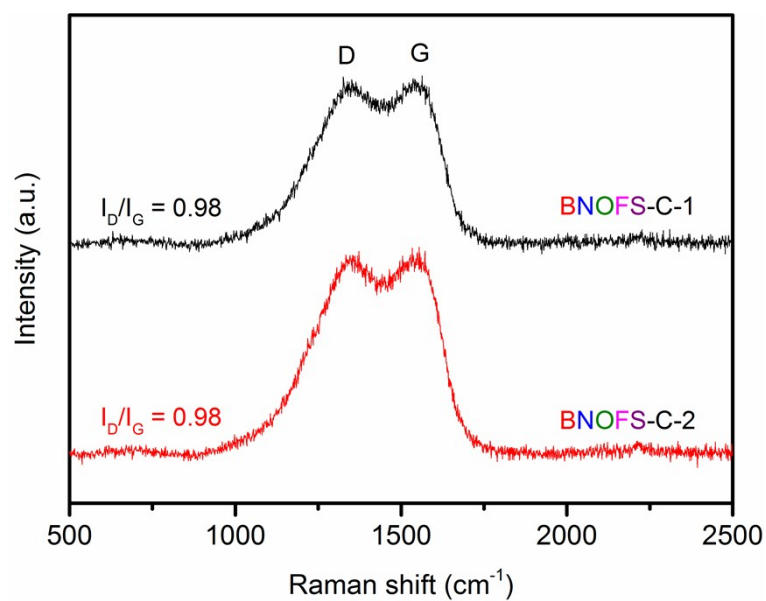
Fig. S7 FTIR spectra of BNOFS-C-1(T) at different temperatures (T) of 400~800°C.
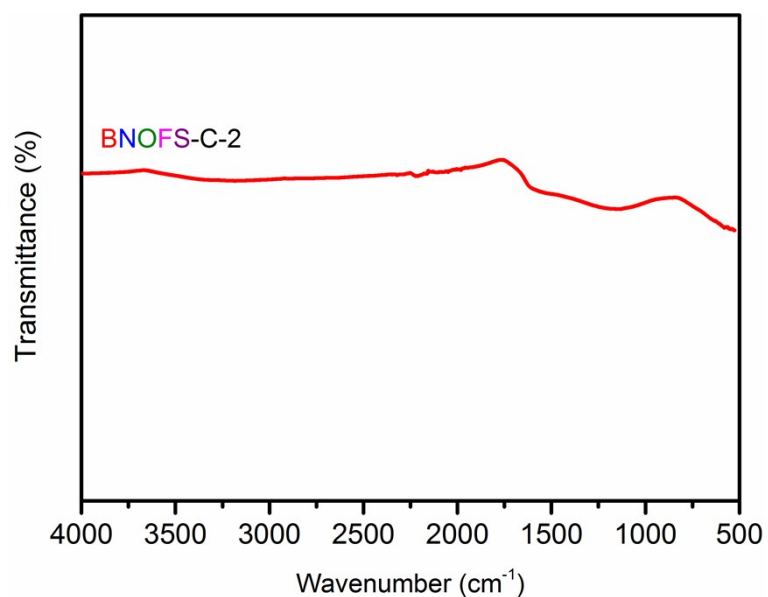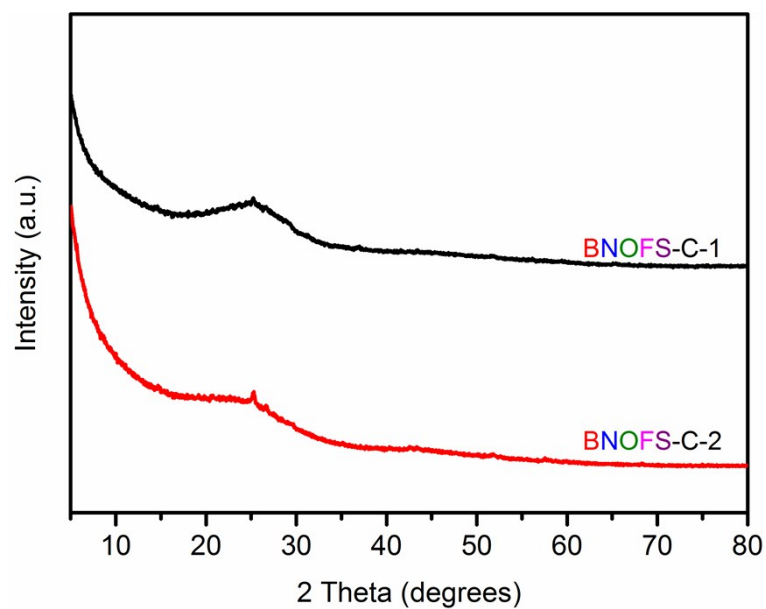

Fig. S8 FTIR spectrum of BNOFS-C-2 at 600°C.
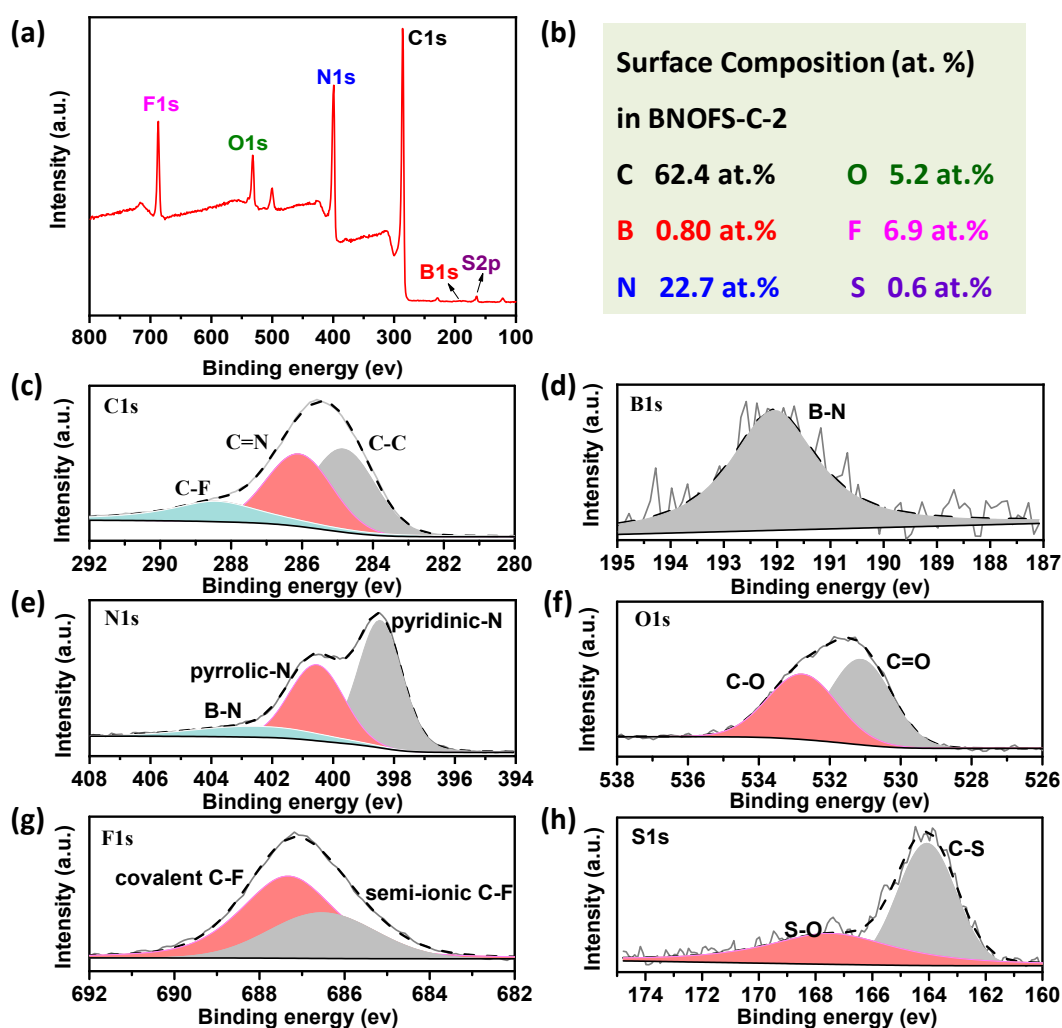
Fig. S9 XPS spectra of BNFSO-C-2. (a) XPS survey spectrum; (b) Surface composition of the elements; (c~h) Spectrum of C1s, B1s, N1s, O1s, F1s, and S2p, respectively.
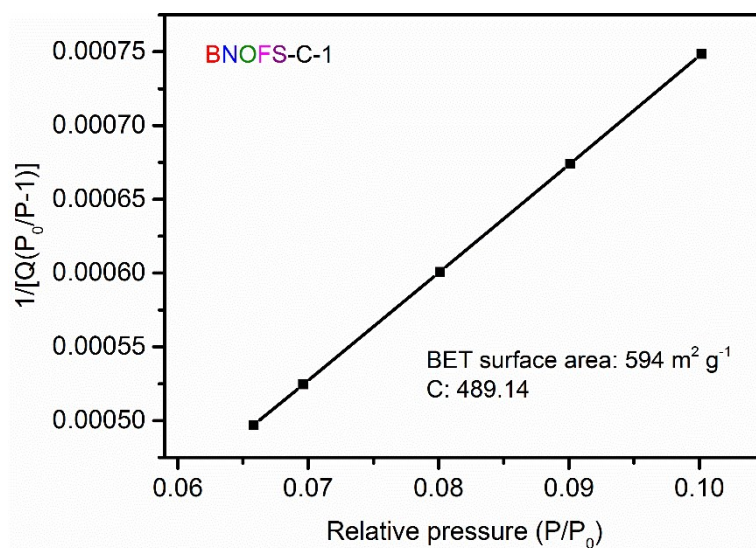
Fig. S10 Raman spectra of BNOFS-C-1 and BNOFS-C-2 with peaks at 1345 cm^{-1} and 1572 cm^{-1} assigned to D band and G band, respectively.
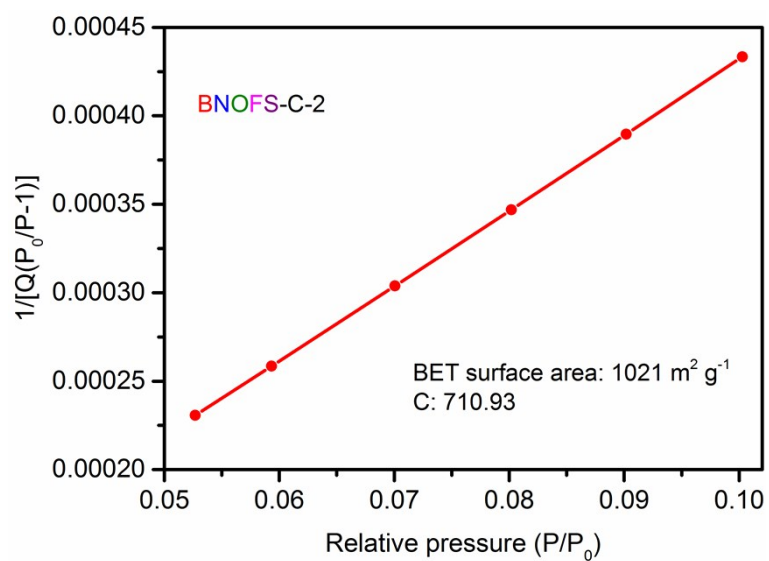

Fig. S11 X-ray diffraction (XRD) patterns of BNOFS-C-1 and BNOFS-C-2.
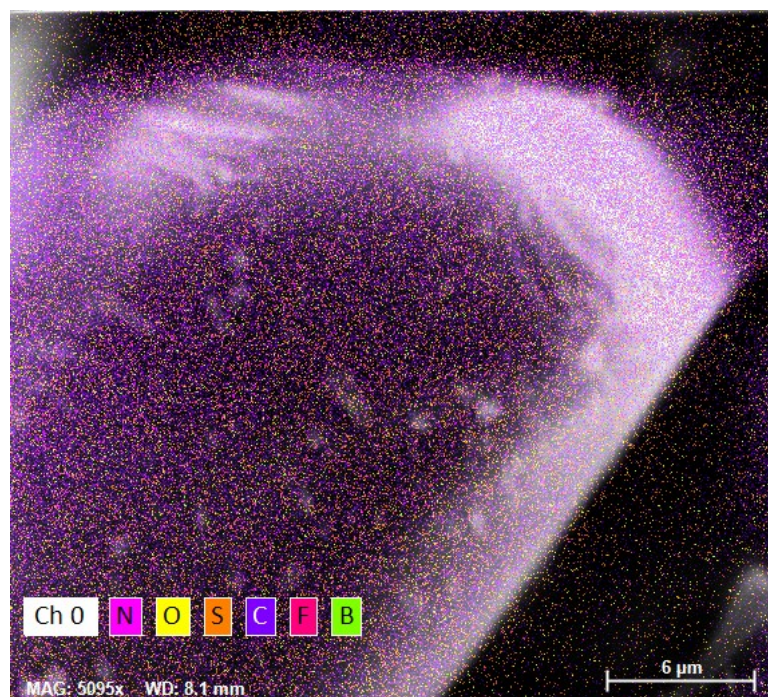
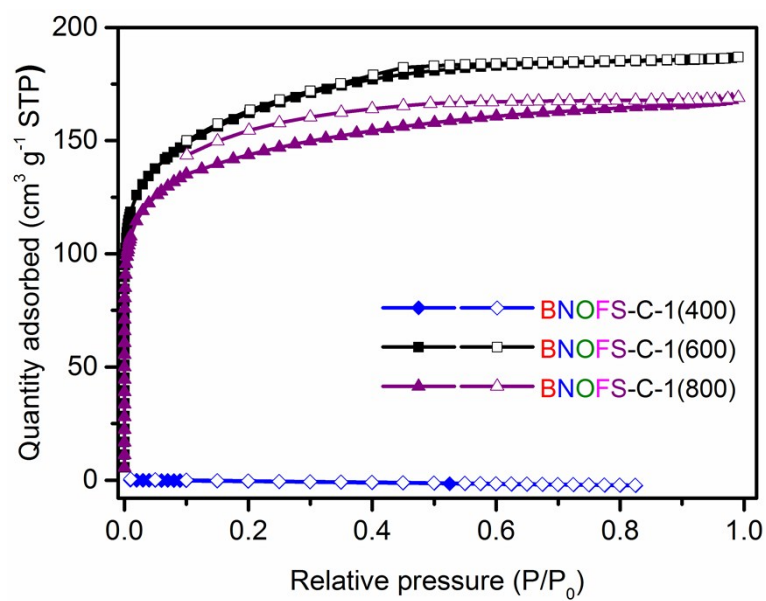**Fig. S12** The total elemental mapping image of BNOFS-C-1.

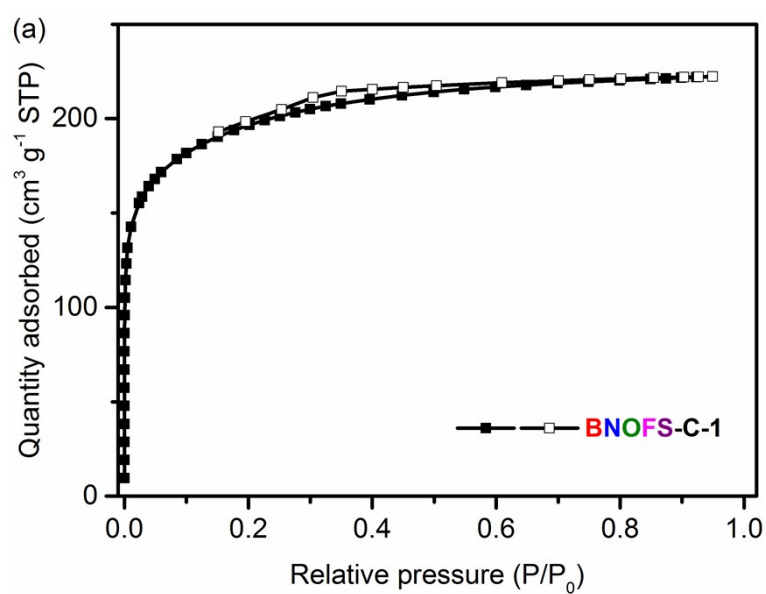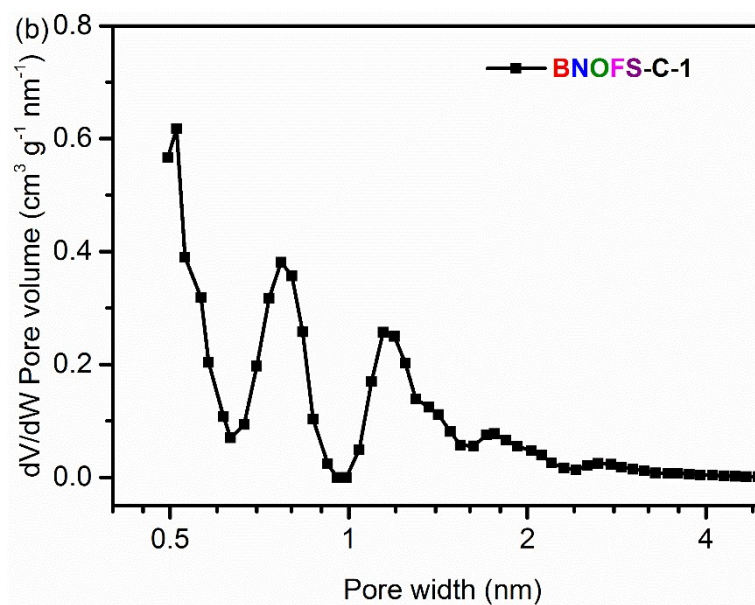**Fig. S13** BET plot for the porous carbon BNOFS-C-1.

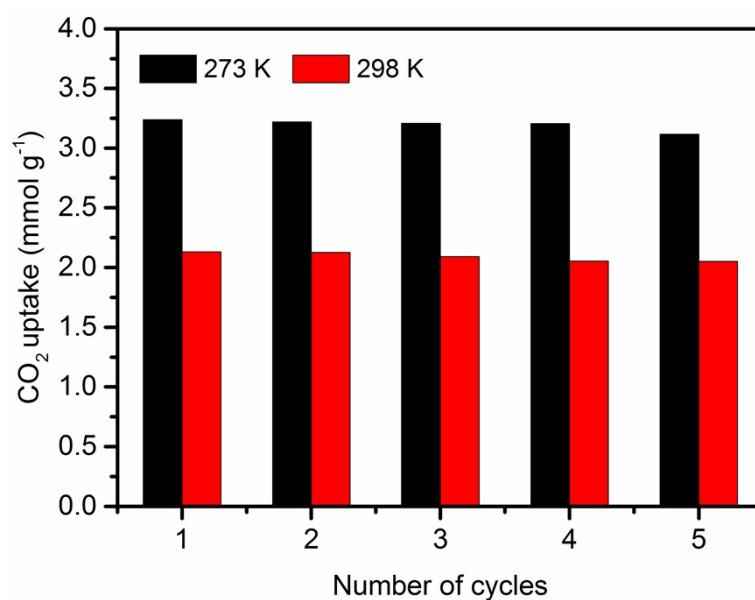**Fig. S14** BET plot for the porous carbon BNOFS-C-2.

Fig. S15 Nitrogen sorption isotherms of BNOFS-C-1 samples obtained at different carbonization temperatures.
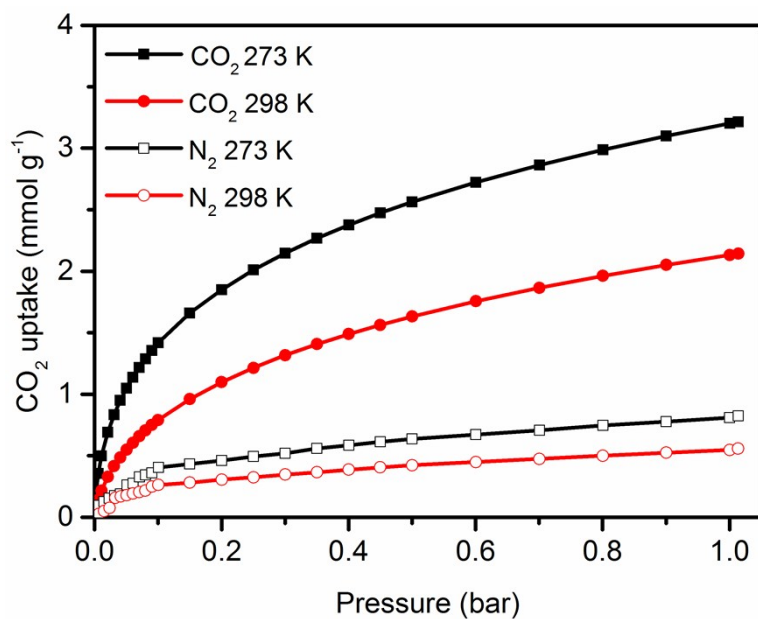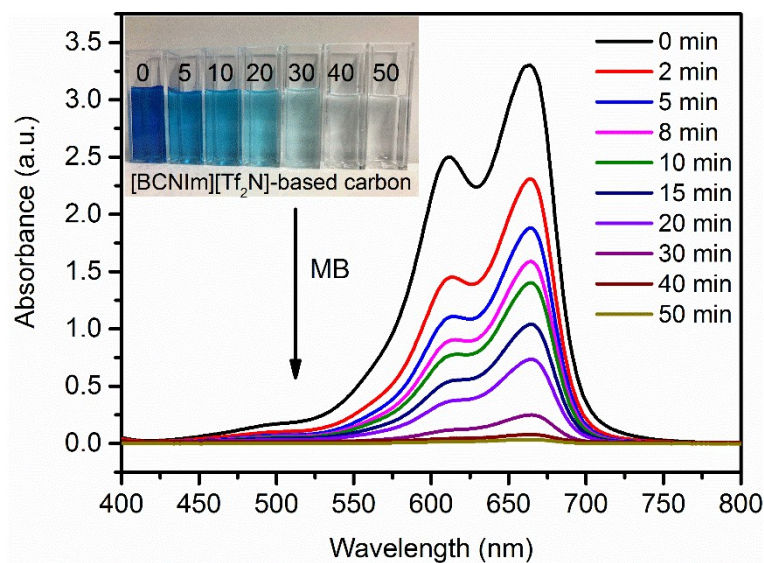
Fig. S16 Argon adsorption isotherms at 87 K (a) and NLDFT pore size distributions (b) of BNOFS-C-1.


Fig. S17 CO_2 adsorption capacity of BNOFS-C-1 at 1 bar in five repeated cycles.

Fig. S18 CO_2 and N_2 adsorption isotherms for BNOFS-C-1.

Fig. S19 Ultraviolet-visible absorption (UV-Vis) spectra of MB aqueous solution treated with [BCNIm][TFSI]-derived porous carbon at different time intervals. The inset photograph shows the corresponding color change of the MB solution. The initial concentration of the MB is 0.05 mM.
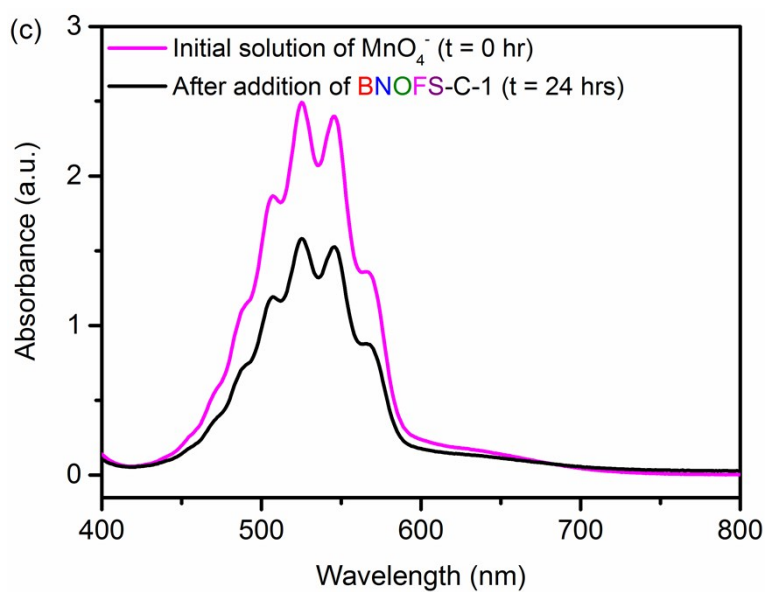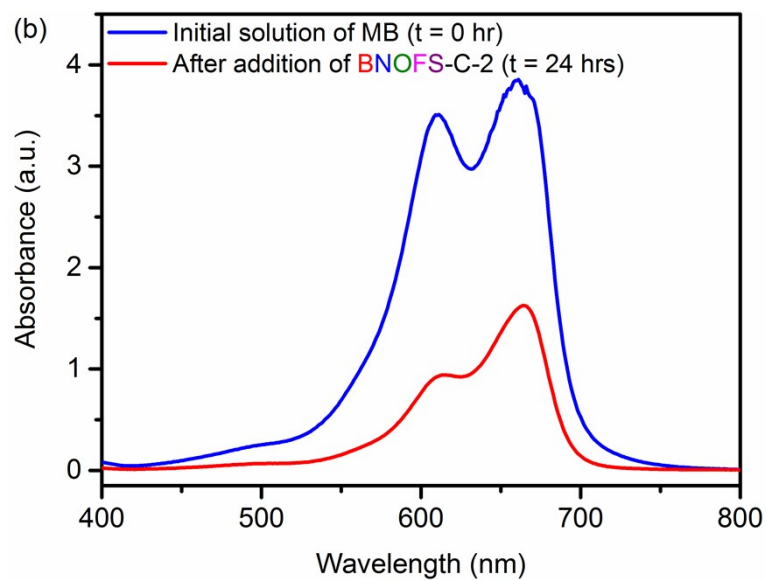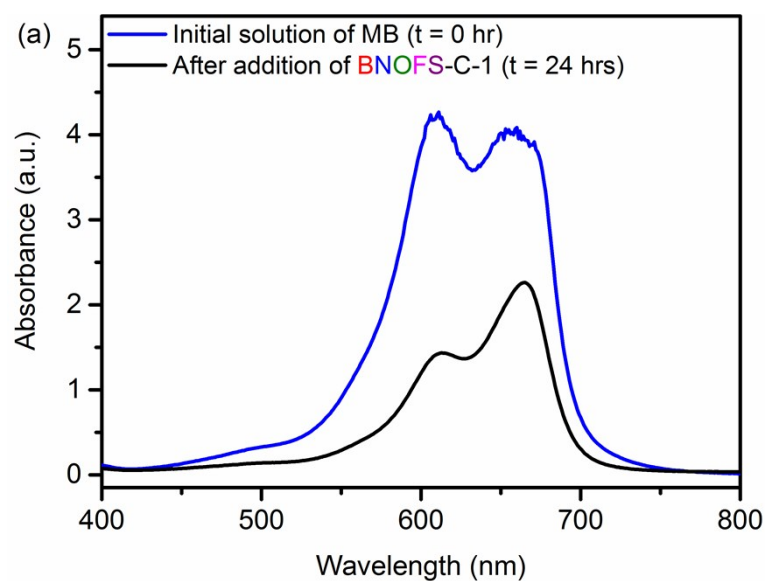
Fig. S20 UV-Vis spectra of dye solution before and after addition of porous carbons (time duration: 24 hrs); The initial concentrations and volume of the MB is 0.1 mM and 10 mL for (a), 0.08 mM and 25 mL for (b). The initial concentrations and volume of the MnO_4^- is 1 mM and 15 mL (c). For all the test, the mass of the porous carbon is 3 mg. Capacity of porous carbons for dye has been calculated from these data.

Reference

1. J. S. Lee, X. Wang, H. Luo, G. A. Baker and S. Dai, *J. Am. Chem. Soc.*, 2009, **131**, 4596-4597.
2. S. Zhang, T. Mandai, K. Ueno, K. Dokko and M. Watanabe, *Nano Energy*, 2015, **13**, 376-386.
3. S. M. Mahurin, P. F. Fulvio, P. C. Hillesheim, K. M. Nelson, G. M. Veith and S. Dai, *ChemSusChem*, 2014, **7**, 3284-3289.
4. J.-S. M. Lee, M. E. Briggs, T. Hasell and A. I. Cooper, *Adv. Mater.*, 2016, **28**, 9804-9810.
5. F. Niu, L. Tao, Y. Deng, H. Gao, J. Liu and W. Song, *New J. Chem.*, 2014, **38**, 5695-5699.
6. R. Shen, X. Yan, Y.-J. Guan, W. Zhu, T. Li, X.-G. Liu, Y. Li and Z.-G. Gu, *Polym. Chem.*, 2018, **9**, 4724-4732.
7. S. Naeem, V. Baheti, J. Militky, J. Wiener, P. Behera and A. Ashraf, *Fibers and Polymers*, 2016, **17**, 1245-1255.
8. F. Chen, M. Hong, W. You, C. Li and Y. Yu, *Appl. Surf. Sci.*, 2015, **357**, 856-865.
9. P. Samanta, P. Chandra, S. Dutta, Aamod V. Desai and S. K. Ghosh, *Chem. Sci.*, 2018, **9**, 7874-7881.
10. N. Mahadevaiah, B. Vijayakumar, K. Hemalatha and B. S. Jai Prakash, *Bull. Mater. Sci.*, 2011, **34**, 1675-1681.